Heliyon 9 (2023) e17794

Contents lists available at ScienceDirect

Heliyon

journal homepage: www.cell.com/heliyon

Studying the effect of reactor design on the electrocoagulation treatment performance of oily wastewater

Muhammad Aiyd Jasim [a], Forat Yasir AlJaberi [b], Ali Dawood Salman [c,d], Saja Mohsen Alardhi [e], Phuoc-Cuong Le [f], Gvendolin Kulcsár [c], Miklós Jakab [g,*]

[a] Samawa Refinery Department, Board of Production, Midland Refineries Company, Ministry of Oil, Al-Muthanna, Iraq
[b] Chemical Engineering Department, College of Engineering, Al-Muthanna University, Al-Muthanna, Iraq
[c] Sustainability Solutions Research Lab, University of Pannonia, Veszprém, Hungary
[d] Department of Chemical and Petroleum Refining Engineering, College of Oil and Gas Engineering, Basra University for Oil and Gas, Basra, Iraq
[e] Nanotechnology and Advanced Material Research Center, University of Technology, Iraq
[f] The University of Danang-University of Science and Technology, Danang, 550000, Viet Nam
[g] Department of Materials Engineering, University of Pannonia, 8201, Veszprém, Hungary

ARTICLE INFO

Keywords:
Electrocoagulation reactor
Finned-cylinder cathode
Petroleum wastewater
Total dissolved solid
Optimization

ABSTRACT

Several conventional methods are employed to remove numerous pollutants from oily wastewater discharged from oil-field activities. The purpose of this study is to use a new design of an electrocoagulation reactor (ECR) to treat oily wastewater effluents from the Al-Muthanna petroleum plant to minimize a Total Dissolved Solids (TDS) to levels suitable for employment. In a continuous ECR, a One-Sided-Finned cathode tube (1SF) made of aluminum was inserted between a pair of aluminum-cylindrical anodes. The effects of the electrolysis period (4–60 min), current density (0.63–5.0 mA/cm^2), and flow rate (50–150 ml/min) on Final TDS value were investigated. The increment of flow rate causes the final TDS value to be increased, while the extending of the electrolysis process and the raise in current density reduces it. The final TDS was 1842.54 mg/l (reduce by 307.46 mg/l) at optimum values of 1-h electrolysis, 5 mA/cm^2 current density, and 50 ml/min flow rate, with an inner anode consumption of 0.13 g and an outer anode consumption of 0.43 g. Regression models with a p-value of 0.001 and F-value of 27.01 noted that the selected model components were important, and the estimated model is considered prominent. Furthermore, the regression coefficient (R^2 = 97.99%) for the final TDS response revealed that the model fit the data well. This study confirmed the ability of the new electrocoagulation reactor to treat petroleum wastewater under significant conditions which overcomes the drawbacks of the conventional designs of electrocoagulation reactors.

1. Introduction

During the extraction and refinement of crude oil, water is employed extensively [1–3]. When crude oil is extracted from underground reservoirs, a lot of generated water is released upstream [4,5]. A greater amount of oily wastewater effluent is released downstream during the refining of crude oil. Aquatic biota are harmed by oil spills and industrial process discharge into bodies of water [6]. Water contamination is still a big issue since it endangers living creatures' health, the environment, and the economy [7]. A

* Corresponding author.
E-mail address: jakab.miklos@mk.uni-pannon.hu (M. Jakab).

https://doi.org/10.1016/j.heliyon.2023.e17794
Received 10 May 2023; Received in revised form 21 June 2023; Accepted 28 June 2023
Available online 4 July 2023

significant amount of water is released as effluent during the refining of oil. Cleaning these effluents lessens pollution and enables water reusing [8].

Substantial amounts of water, also known as produced water (PW), are routinely created during different activities done in oil-field process. PW has both organic and inorganic components [9]. Organic components include hydrocarbons, whereas inorganic ones may include ammonia, cyanide, heavy metals, total suspended solids (TSS), total dissolved solids (TDS), and total organic carbon (TOC) [10]. The high concentration of aliphatic and aromatic compounds in the refinery effluents causes significant harm to the ecology [11]. The TDS term is used to estimate the dissolved organic matter and inorganic salts of aquatic bodies including calcium, chloride, potassium, sulfates, magnesium, sodium and bicarbonates. The increment of TDS level in aquatic systems may occur as a result of human activities such as water use, agriculture, mining, and industry processes. The excess levels of TDS cause toxic to human and aquatic life. The wastewater produced from oil-field activities involving TDS and oil content which is above the average maximum value set by local standards. The average amount of TDS content in oil-field activities is also affected by the age and location of the oil wells. The acidic or semi-neutral solutions, unlike the basic solutions which have a greater value of TDS due to the abundance of different ions in such solution as the time of reaction increases.

Table 1 provides the permissible ranges of TDS in portable water and details when the TDS ranges presented in water is acceptable for drinking or not [7,10].

In refinery effluent treatment, oil-water separation using chemical coagulation process is commonly used prior to the biological treatment [12]. However, these systems had numerous technical and operational drawbacks, as well as significant sludge formation. As a result, a practical and efficient technique for treating the effluents produced by petroleum refineries should be used [3]. Total dissolved solids in these effluents is one of the essential issues in any treatment technologies which are employed to minimize this effect in the contaminated water.

In most cases, using just one method to treat wastewater is insufficient for optimal results. Therefore, a combination of chemical, physical, and biological treatments is the most typical way to treat oily wastewater. The presence of aromatic rings and the high molecular weight of the organics may be the cause of this. A number of elements, such as removal capacity, estimated time to reach the treatment border, alternative pollutants produced, building cost, operating cost, and maintenance cost, have an impact on the effectiveness of the essential processes [13]. Due to the danger that dye molecules pose to living organisms, the biological processing of textile wastewater is inefficient. Adsorption and precipitation are physical processes that require effort and expense. On the other hand, the majority of chemical reactions produce secondary pollutants, like the addition of chlorine and aluminum sulfate. Similar to this, secondary pollutants are produced by other cutting-edge technologies like UV/O_3 or UV/H_2O_2 photo-oxidation [14]. Other methods, like electro-coagulation, have been used to remove contaminants from wastewater [15], which primarily uses electrolytic reactions on the electrode plate to aid in coagulation. Contaminants are removed by dissipating the electric charge brought on by destabilizing elements [16].

Electrocoagulation is an effective wastewater treatment process for finely dispersed particles. EC is a straightforward process with a number of benefits over alternative methods, including the lack of additional chemicals or pricey equipment [9]. The old method's chemical-intensive steps have been replaced with this simple and effective technology [17]. The oxide layer, energy consumption, and sludge generation are all disadvantages of the electrical coagulation technique. In the electrolytic oxidation process, coagulants form in the electrolytic oxidation reaction due to direct current from the anode electrode [18]. Metal ion composites were created by dissolving a "sacrificial anode" with an electrical current. These ions come together to form flocs, which absorb dissolved substances and lessen the stability of colloidal pollutants in wastewater [19,20].

When an electric current is passed between electrodes in EC, redox processes take place. At the anode, oxidation takes place, while at the cathode, reduction happens. Using water analysis, an electric current generates Al^{3+} ions on the anode's surface, which react with OH^- ions on the cathode to create solid $Al(OH)_3$ agglomeration. O_2 and H_2 gases are simultaneously emitted near the anode and cathode, respectively. These gases promote flotation, which causes flocs to rise to the liquid's surface and lighter objects to sink (Eqs. (1)–(5)) [10,21].

$$Al_{(s)} \rightarrow Al^{3+}_{(aq)} + 3e^- \quad (1)$$

$$2H_2O \rightarrow O_2 + 4H^+ + 4\,e^- \quad (2)$$

$$2H_2O + 2e^- \rightarrow H_{2(g)} + 2OH^-_{(aq)} \quad (3)$$

$$Al^{3+}_{(aq)} + 3OH^- \rightarrow Al(OH)_3 \quad (4)$$

$$nAl(OH)_3 \rightarrow Al_n(OH)_{3n} \quad (5)$$

Table 1
TDS ranges and details of acceptance.

TDS ranges (ppm)	Details
Less than 50	Unacceptable because it has less crucial minerals
50–150	It is good for areas where the aquatic systems polluted by industrial waste or sewage
150–350	Good
350–1200	Least acceptable
Above 2000	Unacceptable

Electro-coagulants are formed based on different ions released throughout the electrocoagulation reactor that help in trapping or adsorbing the pollutants [22,23]. The electro-generated coagulants better than chemical coagulants due to their larger size than chemical coagulants, have a small pH range at which they are soluble, and are easily separated [24]. The usage of electrocoagulation process to remove pollutants from produced wastewater [25,26], effluents from the textile industry [27,28], heavy metals from oily wastewater, including zinc and copper [29,30], chromium in tannery waste [31], color removal from sugar beet molasses [32], phosphate derived from mining effluents [33] has all been applicable.

As known, the electrochemical cell's oxidation process moves more quickly than its reduction process, which results in a significantly larger release of aluminum ions from the anode than hydroxyl ions from the cathode. As a result, the cathode's surface area should be increased while minimizing the volume of the reactor. Since the oxidation process is more rapid than the reduction process throughout the EC cell, which means that the release of Al ions from the anode is much than the release of OH ions at the cathode, therefore, the surface area of the cathode has been maximized without excessive enlargement of the reactor's volume. This study attained the solution to this issue via the employment of multi-fins at the outer surface of the cathode with a significantly small wet volume of the reactor. As a result, the amount of OH ions has been increased, more electro-coagulants are generated incorporated with aluminum ions, and consequently higher removal efficiency of pollutants is attained. As a result, more electro-coagulants containing aluminum ions will be produced, increasing the number of hydroxyl ions and raising the removal efficiency of contaminants. In order to lower the total dissolved solids (TDS) in petroleum wastewater discharged from the Al-Muthanna petroleum facility, this study intends to deploy this new reactor. With this contemporary method, it also seeks to measure electrode exhaustion while being affected by operational factors (applied current, reaction time, and flow rate) that are more efficient. Application of the (RSM-BBD) and Minitab software for experimental design, analysis, and optimization.

2. Materials and methods

2.1. Petroleum wastewater

The Al-Muthanna petroleum refinery's effluent discharge point was employed to collect the petroleum wastewater used in this investigation (Table 2) and a continuous reactor was employed to handle. The leadership of the refinery estimates that this factory produced approx. 96 m^3/day of effluents every day.

The continuous electrocoagulation process actual electrode consumption (ACE) was calculated using Equation (6) below [9,34]:

$$Actual\ Consumption\ of\ Electrodes\ (AEC) = W_1 - W_2 \quad (6)$$

where W_1 represents the electrode mass before the trial and W_2 represents the electrode mass after the trial [35].

2.2. Electrocoagulation reactor

A DC-supply was used (YX-305D, Yaxun, China) to keep a constant current while allowing for voltage fluctuations with experiment time. The EC reactor was made of plastic and held 2.5 L. In this experiment, an electrocoagulation reactor with three concentric electrode tubes was used. The cathode electrode was located in between the outer and inner anode electrodes. A plastic sedimentation tank of 2.5 L in the shape of a cylindrical bowl with a conical base and a plastic cover that supports a set of 5 baffles plates (length 10 cm, height 2 cm, and thickness 0.2 cm) in series mode. The sedimentation tank separates the oil content from the cleaned water using gravitation and the difference in densities where the water is heavier than the oil content. A diagram of the electrode configuration and electrocoagulation reactor is shown in Fig. 1. An aluminum One-Side Finned (1SF) tube cathode contains 27 fins, the space between each fin 0.4 cm, and each fin are divided at its terminal end into 3 small fins with an entire area of 2185 cm^2. A total surface area of 425 cm^2 of tubular aluminum anodes surround the cathode, one on the outside and one inside. These anodes were inserted into wastewater at a depth of 7.5 cm. The 319 cm^2 active area is used when moisture volume refers to the area of the anodes submerged in water. The distance between the inner and outer anodes and the cathode was 1 cm, but the distance between the two was 2 cm. In this research, total dissolved solids (TDS) was chosen as the analyzed indicator. A conductivity meter (conductivity meter -HM DIGITAL, Korea) was used to measure TDS ions presented in PW.

Since the oxidation and reduction processes are taking place at the anode and the cathode electrodes, respectively, so the anode electrode is eroded to discharge Al ions and materials are deposited on the surface of the cathode. A sandpaper (type: extra fine 280–320) was performed for the cathode only to remove any compounds generated or adsorbed on its surface as a result of the electro-deposition influence during the electrocoagulation process. Otherwise, the anode electrode was cleaned using a rough-brush and washing it by diluted hydrogen chloride acid and distilled water. By the way, the estimation of the electrodes consumption prior and after each run was conducted after the cleaning procedure to obtain the real value of electrodes consumption. But in general, the cleaning process was conducted carefully to keep electrodes safe as possible.

Table 2
Characterization of petroleum wastewater.

Variables	(OC) (mg/l)	TDS (mg/l)	Conductivity (μs/cm)	pH
Values	1870.41	2150	4267	8.1

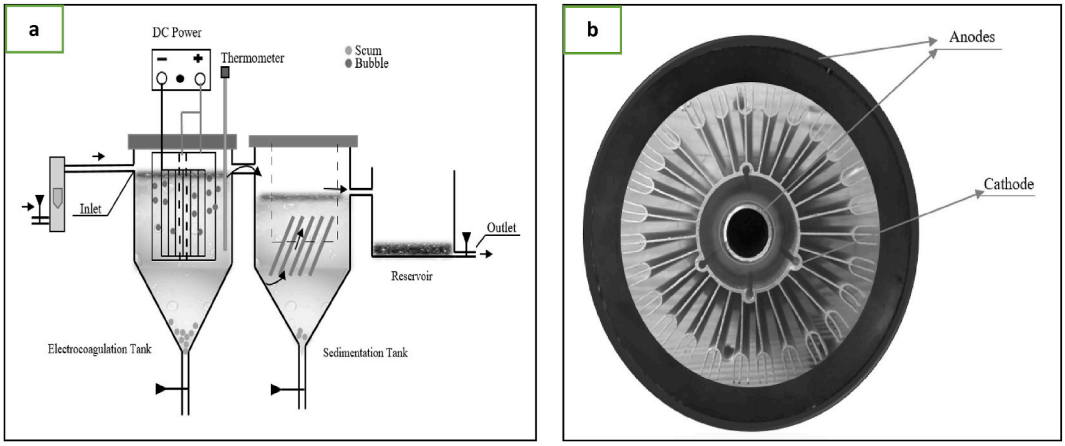

Fig. 1. A diagram showing (a) the electrocoagulation cell and (b) the arrangement of the electrodes.

2.3. Experimental design

The Box-Behnken response surface methodology (RSM-BBD) and Minitab, a statistical tool, were used to plan, analyze, and modify the electrocoagulation investigations. A mathematical relation between the studied response and the operating variables can be presented in a second-order (quadratic) equation (Equation (7)). The regression coefficient (R^2) value and the analysis of variance (ANOVA) results define how the obtained model will fit well to the RSM-BBD designed data with the confidence level of 95% [36,37,43].

$$Y = B_0 + \sum_{i=1}^{q} B_i X_i + \sum_{i=1}^{q} B_{ii} X_i^2 + \sum_{i} \sum_{j} B_{ij} X_i X_j + \varepsilon \quad (7)$$

where Y is the examined answers, expressed as the Final TDS value, and X_1, X_2, to X_q are the operational factors, q denotes all operational parameters, and Bo to Bij are the coefficient vectors.

In this work, the effects of current density CD (X_1: 0.630–5.00 mA/cm2), electrolysis time (X_2: 4–60 min), and flow rate (X_3: 50–150 ml/min) were investigated. To enhance the detected responses, design experts recommended 12 experimental investigations with 3 centroids, notably employing RSM-BBD.

3. Results and discussions

Table 3 shows the actual inner and outer tubular electrode consumption along with the experimental and predicted final TDS values based on real values (and coded values) of the operating variables.

The experimental values of final TDS are shown as points on the fitted line in Fig. 2. As a result, the final TDS projected values show very little variance from the fitted line. This indicates that there is little random error between the experimental and anticipated values of TDS. Points above the line show a positive residual, meaning that the predicted values are higher than the observed values. Points

Table 3
The findings of the variables investigated.

Run	X_1: CD (mA/cm^2)	X_2: Electrolysis time (min)	X_3: Flow rate (ml/min)	Experimental TDS	Predicted TDS	Inner Anode Consumption (g)	Outer Anode Consumption (g)
1	0.630(−1)	4(−1)	100(0)	2207	2180	0.001	0.010
2	5.000(+1)	4(−1)	100(0)	2165	2173	0.001	0.010
3	0.630(−1)	60(+1)	100(0)	2117	2109	0.030	0.110
4	5.000(+1)	60(+1)	100(0)	1938	1965	0.060	0.150
5	0.630(−1)	32(0)	50(−1)	2130	2143	0.030	0.070
6	5.000(+1)	32(0)	50(−1)	2059	2037	0.060	0.120
7	0.630(−1)	32(0)	150(+1)	2265	2287	0.030	0.050
8	5.000(+1)	32(0)	150(+1)	2254	2241	0.050	0.080
9	2.815(0)	4(−1)	50(−1)	2186	2200	0.001	0.020
10	2.815(0)	60(+1)	50(−1)	1895	1890	0.070	0.210
11	2.815(0)	4(−1)	150(+1)	2198	2203	0.010	0.010
12	2.815(0)	60(+1)	150(+1)	2247	2233	0.060	0.070
13	2.815(0)	32(0)	100(0)	2066	2073	0.050	0.120
14	2.815(0)	32(0)	100(0)	2082	2073	0.060	0.100
15	2.815(0)	32(0)	100(0)	2070	2073	0.050	0.110

below the fitted line denote a negative residual, meaning that the predicted values are less than the observed values. The observed final TDS values, which in Fig. 2 range from 1895 to 2265, match the expected values of 1890–2287.

The mathematical relationship between the examined responses

The mathematical correlation (Equation (8)) shows final TDS can be predicted based on experimental data by examining the relationships between operating variables in terms of practical parameters. The perfect agreement between the variable response values and the created TDS models and the peak values of the regression factors serve as indicators of how well the model fits; the bigger the value of the regression parameter, the better the model fits [38]:

$$Y = 2527.1 - 60.1\,X_1 - 6.53\,X_2 - 5.76\,X_3 + 8.33\,X_1^2 - 0.0073\,X_2^2 + 0.02582\,X_3^2 - 0.560\,X_1{*}X_2 + 0.137\,X_1{*}X_3 + 0.06071\,X_2{*}X_3\ (R^2 = 0.9799;\ R^2\ (Adjusted) = 0.9437) \quad (8)$$

Degrees of freedom were taken into account using the adjusted coefficient of regression (Adjusted R^2). The final TDS response's high regression coefficient (0.9799) and the model's (R^2 -adj) value of (0.9437) suggest that the model offers a strong match to the data [9].

3.1. Analysis of variance (ANOVA)

Analysis of variance (ANOVA) was employed as a technique of analysis to match the function to the data since it is crucial to evaluate the quality of the model matched [34,43].

Table 4 displays the findings of the analysis of variance for the final TDS levels. P-values less than 0.050 highlight the significance of specific model components, whereas p-values more than 0.100 show that regression models are statistically insignificant. The calculated model is impressive in the current investigation because the value of F for TDS is 27.07. High values of the regression coefficient for a response also signify the model's applicability and acceptability of the updated R2-adjusted value. Additionally, the (Lack-of-Fit) p-value was higher than 0.05, demonstrating the statistical significance of the current model, which successfully fits the data. The ANOVA results reveal that this model demonstrated the efficiency of the electrocoagulation method in removing pollutants from oily wastewater.

Process parameters' impact on final TDS Response

Fig. 3 depicts the effect of process parameters on final TDS response in a case of other variables' mean values.

As a rule of thumb, the oxidation process is more rapid than the reduction process throughout the EC cell, which means that the release of Al ions from the anode is much than the release of OH ions at the cathode, therefore, the surface area of the cathode has been maximized without excessive enlargement of the reactor's volume. This study attained the solution to this issue via the employment of multi-fins at the outer surface of the cathode with a significantly small wet volume of the reactor. As a result, the amount of OH ions has been increased, more electro-coagulants are generated incorporated with aluminum ions, and consequently higher removal efficiency of pollutants is attained.

3.1.1. The effect of current density

The quantity of different ions released from electrodes and, consequently, the rate of pollutants removal are both impacted by current density, making this operating variable as the most important to consider throughout the electrocoagulation process [39,40].

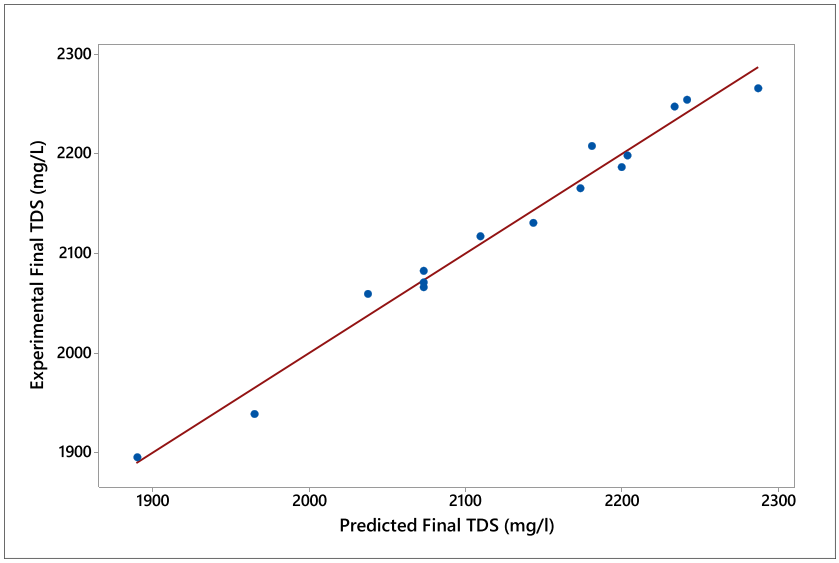

Fig. 2. Experimental and predicted values for final TDS.

Table 4
ANOVA test outcomes for final TDS value.

Source	Degree of Freedom	Sum of squares	Mean square	F-Value	P-Value	
Model	9	165,766	18418.4	27.07	0.001	significant
X_1	1	11,476	11476.1	16.87	0.009	significant
X_2	1	39,060	39060.1	57.42	0.001	significant
X_3	1	60,205	60204.5	88.50	<0.0001	highly significant
X_1^2	1	5846	5846.3	8.59	0.033	
X_2^2	1	120	120.3	0.18	0.692	
X_3^2	1	15,381	15380.8	22.61	0.005	
X_1*X_2	1	4692	4692.3	6.90	0.047	
X_1*X_3	1	900	900.0	1.32	0.302	
X_2*X_3	1	28,900	28900.0	42.48	0.001	significant
Error	5	3401	680.3			
Lack-of-Fit	3	3263	1087.6	15.69	0.061	
Pure Error	2	139	69.3			
Total	14	169,167				

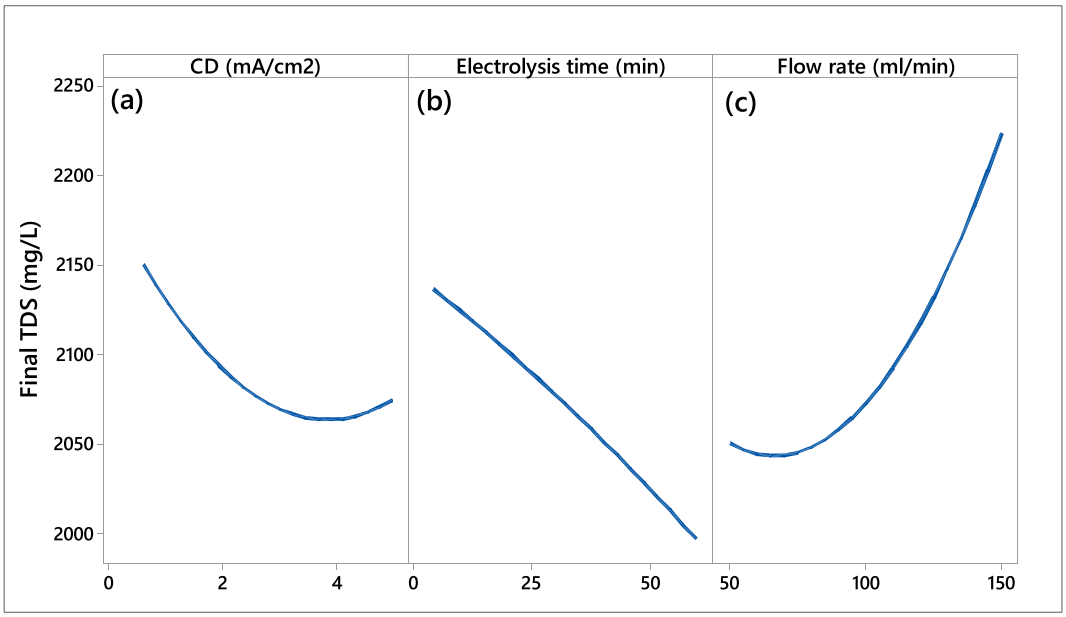

Fig. 3. The impact of the operating parameters on the final TDS. (a) Current density (mA/cm^2), (b) the electrolysis time (min), and (c) flow rate (ml/min).

Electrochemical coagulation technology is always dependent in its process on the generation of coagulants due to the continuous supply of electric current without any addition of chemical additives to decrease the amount of TDS. The generation of these coagulants in the ECR will impact the behavior of TDS' response. Therefore, the concentration of TDS may be altered according to several influences, such as the performance of the electrocoagulation reactor, electric current applied, and the configuration of electrodes and their active area.

To study the effects of current density on EC reactor performance. Fig. 3a illustrates the correlation among final TDS removal and current density at a flow rate of 100 ml/min and a mean reaction period of 32 min. The findings led to a decrease in TDS from 2117 mg/L at 0.630 mA/cm2 to 1938 mg/L at 5.000 mA/cm2. Increased current density makes it easier for the anode to produce enough adsorbents to remove contaminants from the solution, and the cathodic active area of the current design helped produce the extra hydroxyl ions required to produce more electro-generated coagulants, which increased TDS removal [36,41]. The results can be explained by the fact that the amount of TDS decreases with increasing current density, yet the reaction gradually increases at high current density values. The efficiency of removing contaminants from wastewater behaves similarly to what [14,23] have observed. The mathematical relationship between the average values of various variables and the final TDS response to the current density is shown in Equation (9):

$$Y = 1490\ X_1 - 220.4\ X_1^2\ R^2 = 0.88 \quad (9)$$

3.1.2. The influence of electrolysis time

The response time is one of the most important operational elements that directly influences how well an electrocoagulation reactor performs [12]. The amount of time the solution volume where the electrodes are located is in contact with the current electrodes during the electrolysis process, as stated in the EC section, is referred to as the electrolysis time in this work. The duration of the treatment procedure should be evaluated in order to estimate how long it will take to produce a sufficient amount of electro-coagulants for adsorption-based pollutant elimination from petroleum wastewater [42]. Fig. 3b clearly shows that as the electrolysis time increases, the final TDS response rapidly drops. As the reaction time increases, these contaminants are removed from the diluted solution due to the electrocoagulation cell's adsorption and desorption processes [26]. During the electrocoagulation process, the electro-generated $Al(OH)_3$ and impurities hetero-aggregated as a result of the electrostatic contact between the negatively charged particles. The various kinds of aluminum ion composites produce flocculent when they react with TDS in wastewater. The synthesis of aluminum ionic composites will grow with increased reaction time, and as a result, the wastewater's anions will be balanced. Based on the core observations that the TDS elimination efficiency improves as the reaction time increases. The finned design of the cathode provides an adequate amount of electro-generated coagulants for treating the solution [9]. An extremely higher rate of gas-bubble generation at electrodes and the formation of passivation effect on the electrode will reduce the destabilizing pollutant rate and removal efficiency, decreasing this behavior. But the positive effect of these bubbles formed among fins will formed many of tiny eddies that will assist the agitation process throughout the EC reactor.

This discovery is identical to what [10,24] stated. Equation (10) illustrates the mathematical relationship between the final TDS response and the electrolysis time when other variables have mean values:

$$Y = 122.4\ X_2 - 1.503\ X_2^2 R^2 = 0.816 \tag{10}$$

3.1.3. Effect of flow rate

Fig. 3c shows that the wastewater flow rate also has a significant influence on TDS removal. When the wastewater flow rate is altered, the electrolysis time in the EC reactor—which houses the current electrodes—changes. The flow rate, which varied from 50 to 150 ml/min, was chosen as an operating factor because the chemical reactor's current design distinguishes itself by a continuous operation mode. TDS behavior alters when the flow rate changes, as demonstrated. When flow rates are low, it decreases with increasing flow rates; however, when flow rates are high, Due to the pollutant reduction process' failure to allow enough time for the pollutants to adsorb on the different ions and the passing of some of the solution outside without reaction, the TDS response increases rapidly with rising flow rates [14] came to a same conclusion. Equation (11) shows the mathematical relationship between the final TDS response and flow rate given the median rates of other variables:

$$Y = 42.15\ X_3 - 0.1878\ X_3^2 R^2 = 0.98 \tag{11}$$

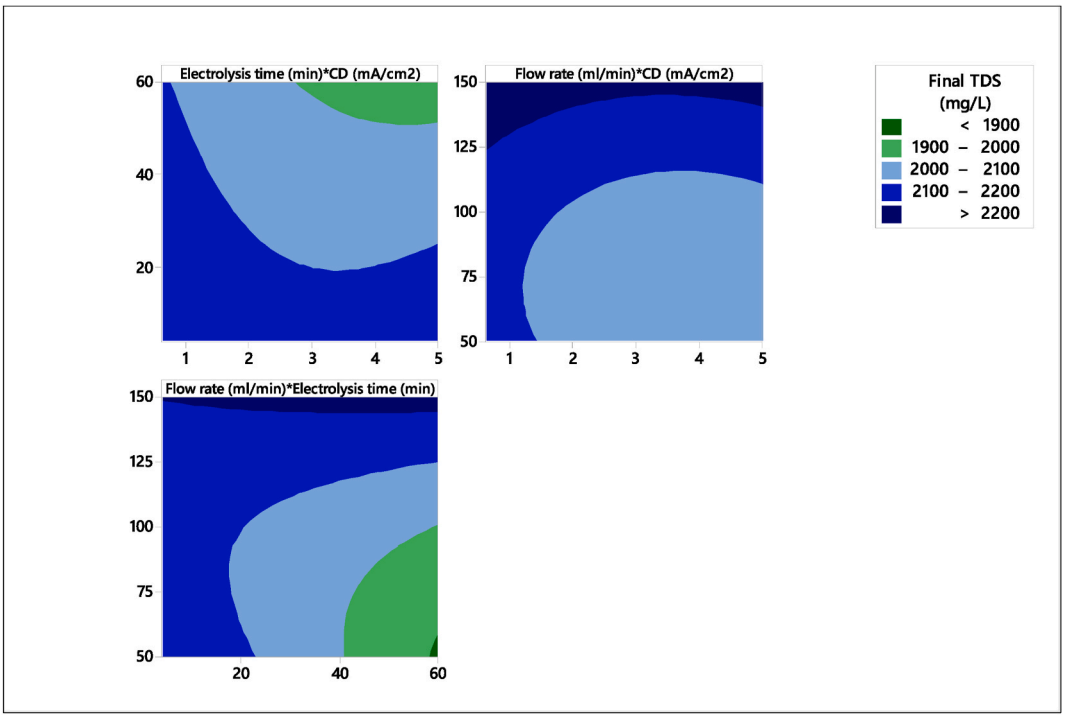

Fig. 4. The final TDS response vs. the Contour plots of the studied variables. (a) current density-electrolysis time pair (b) current density-flow rate pair (c) electrolysis time-flow rate pair.

The TDS value is associated with the anode's release of aluminum ions. The dissolution of aluminum ions depends on the flow rate, electrolysis time, and current density. This demonstrates that dissolved solids tend to diminish or grow depending on the electrode's real consumption and the amount of dissolved salts. When the emissions of aluminum ions are high and considerably bigger than the pollutants in the solution, the TDS response begins to increase at high current density values, and also when the amount of dissolved salts is high, it increases TDS at high flow rates. Fig. 4 depicts the major effect of each pair of operational parameters on the final TDS response by the contour plots, where the other variable is held constant at its mean value for each case while each pair is adjusted according to the planned range, e.g., 32 min of electrolysis time, 2.815 mA/cm^2 of current density, and a flow rate of 100 ml/min. According to the behavior of TDS response shown in the (contour plot), the electrolysis time-flow rate pair has a noticeably bigger impact than the current density-electrolysis period pair and the current density-flow rate pair. These results matched those of the ANOVA test well, as shown in Table 4.

3.2. Consumption of electrodes

3.2.1. Inner anode consumption

Equation (6) was used to calculate the electrical exhaustion of anodes for the factors studied. The following objectives will be investigated based on Fig. 5 to evaluate the impact of process factors on the inner anode consumption response in the case of other variables' mean values.

The relationship between the inner anode consumption response, current density, and electrolysis time is depicted in Fig. 5a and b. According to the findings, the internal anode consumption increased gradually with increasing current density and rapidly with increasing electrolysis time. The response then gradually slows down when it reaches the middle values and tends to diminish at high values. Fig. 5c depicts the inner anode consumption response as a function of flow rate. As flow rates increased, they slowly decreased.

3.2.2. Outer anode consumption study

The following objectives will be investigated based on Fig. 6 to evaluate the impact of process factors on the outer anode consumption response in the case of other variables' mean values. Fig. 6a and b show the relationship between outer anode consumption response, current density, and electrolysis time. According to the findings, the outer anode consumption increased gradually with increasing current density then gradually slows down when it reaches the middle values and tends to diminish at high values. But it increased rapidly with increasing electrolysis time. Fig. 6c depicts the outer anode consumption response as a function of flow rate. As flow rates increased, they slowly decreased.

The results can be explained by the fact that larger concentrations of pollutants require more adsorbents at the beginning of the experiment due to the release of various ions from the electrodes; therefore, when there is an excess of adsorbents, the dissolution of the electrodes is reduced. Actual consumption of electrodes increased and declined gradually due to the active area supplied by the novel electrode's current design and greasy wastewater's electrical conductivity. The formation of an oxide layer on the anode surface slows the anode decomposition process. The considerable effect of the same variables on electrode consumption was documented by Refs. [10,14].

3.3. Effect of each electrode's consumption on the final TDS value

In accordance with Fig. 7, the purposes that follow will be investigated to assess the impact of inner and outer anode consumption

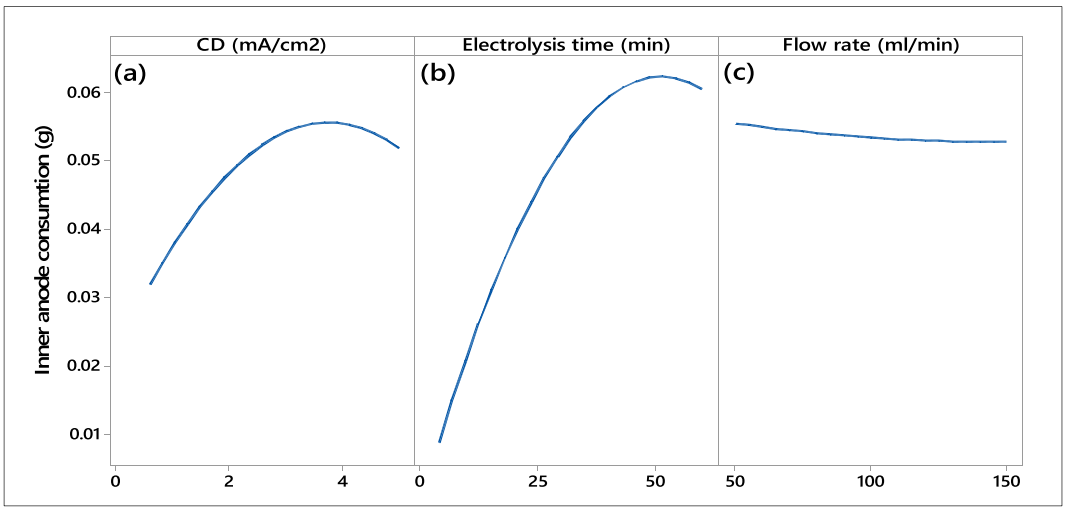

Fig. 5. The impact of the operating parameters on Inner Anode Consumption. (a)Current density (mA/cm^2), (b) the electrolysis time (min), and (c) flow rate (ml/min).

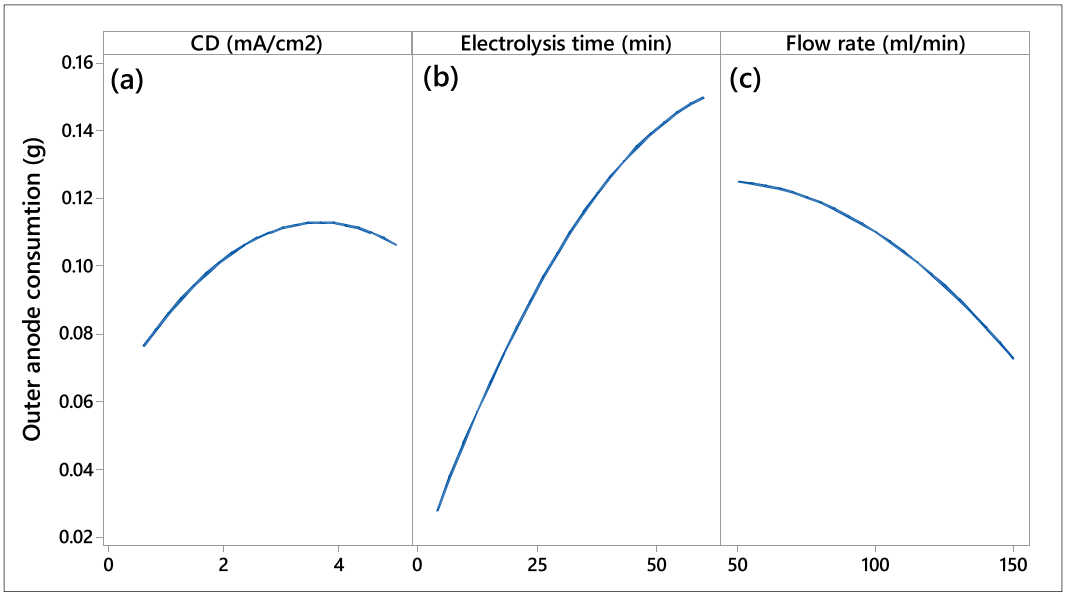

Fig. 6. The impact of the operating parameters on Outer Anode Consumption. (a) Current density (mA/cm^2), (b) the electrolysis time (min), and (c) flow rate (ml/min).

on the final TDS response.

The relationship between the final TDS response and the internal and external anode consumption is depicted in Fig. 7. Electrode consumption is an important factor in electrocoagulation because it controls the rate at which pollutants are removed by ions discharged from the electrodes. According to the findings, the effect of consuming the outer electrode on the final TDS value is greater than the effect of consuming the inner electrode due to the careful design of the cathode, which provides a larger surface area than the outer side due to the presence of fins, which aids in the release of a larger amount of hydroxide that combines with the aluminum ion, forming a large amount of adsorbent. To remove impurities from a solution.

Fig. 8 shows the significant effect of the internal and external anode consumption pair on the final total dissolved solids. The final TDS response behavior shown in Fig. 8 showed that the inner and outer anode consumption pair has a significant influence on the TDS value, with the increase of electrodes consumption, the final TDS value will decrease. These results were in good agreement with those obtained by ANOVA test shown in Table 4.

Based on the results of the experiments, Table 5 shows the mathematical correlations of inner and outer anode consumption, operational variables in aspects of precise factors for calculating electric inner and outer anode consumption (Equations (12) and (13)).

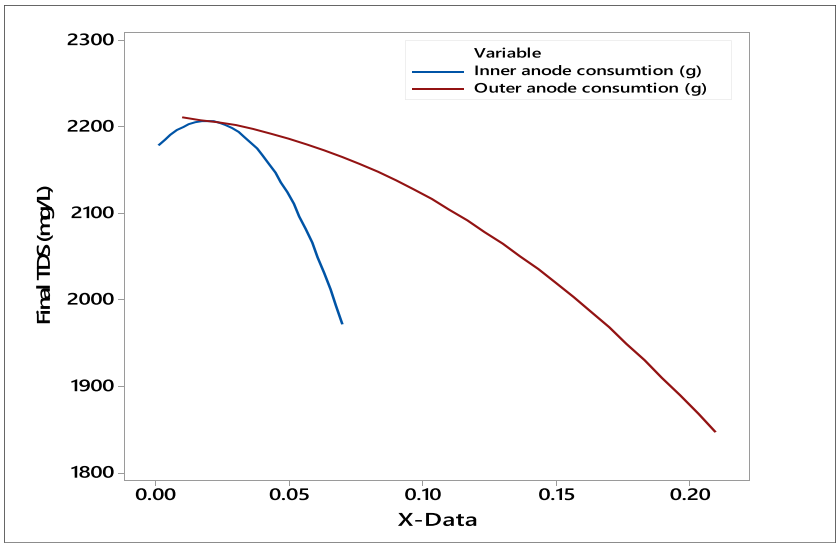

Fig. 7. The influence of the inner and outer anode consumption on the final TDS response.

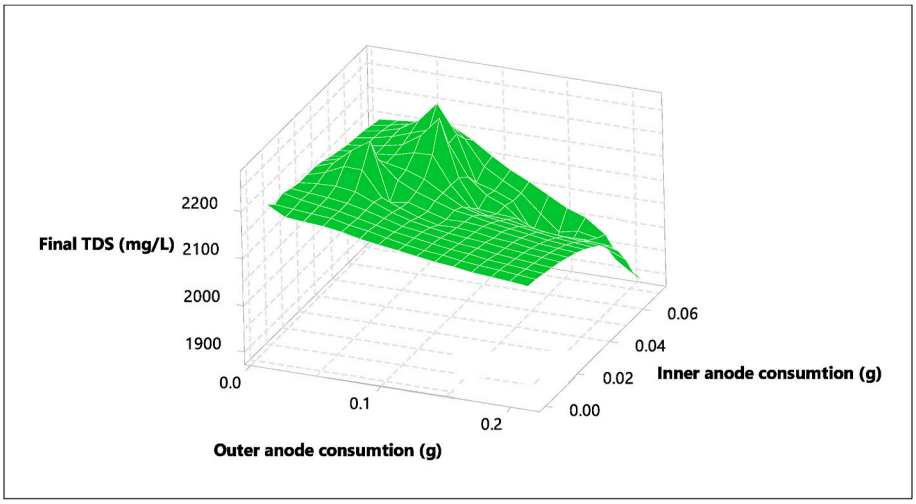

Fig. 8. The influence of pair of the inner and outer anode consumption on final TDS.

Peak regression factor values and the perfect convention between variable response values expenditure of electrode models are indicators of model fit. The high regression coefficient values (0.9184 and 0.9142) for inner and outer anode consumption responses indicate that the model fits the data well and is consistent with the (R^2 -adj) values of 0.9709 and 0.9694.

3.4. Optimization of operating parameters

Statistic software (Minitab-18) was used to assessment the optimization steps. The acquired feedbacks are precise when D equals 1, as shown in Fig. 9. One hour of electrolysis at a current density of 5.0 mA/cm^2 and a flow rate of 50 ml/min was optimal for reduced of the final TDS to 1842.54 mg/l. The study's main results suggested that petroleum wastewater may be processing using a newly designed electrocoagulation reactor to remove TDS. Due to the favorable impact of larger fins, optimum process factor values, essentially electrolysis period and current density, were lower than in prior research.

According to Fig. 9, the optimum flow rate was the lowest achievable value for the reason that increasing the flow rate causes the drainage of unprocessed solution to increase because the solution's holding time in the reactor shortens, affecting the necessary interplay between the ions in the solution. To guarantee the emission of several ions necessary for a compilation of electro-coagulants, a higher current density and electrolysis period might be advantageous. Under ideal circumstances, 0.56 g of actual electrode consumption was consumed.

4. Conclusions

The state-of-the-art electrocoagulation apparatus has been tested for its ability to remove TDS from the Muthanna petroleum refinery effluent. 1 h, 5 mA/cm^2, and 50 ml/min proved to be the optimum reaction period, current density, and flow rate, respectively. As mentioned above, the main factors affecting the removal of TDS are current density and electrolysis period. The removal improves as the current density and response time ramp up to 5000 mA/cm^2 and 1 h, respectively. The elimination of TDS decreases when the flow rate is increased. According to the findings, the effect of consuming the outer electrode on the final TDS value is greater than the effect of consuming the inner electrode. Higher regression coefficients ($R^2 = 97.99\%$) and ANOVA analyses of the data show that the quadratic polynomial model has been appropriately modified. Comprehensive, the results of the research showed that the innovative design of the electrocoagulation reactor is dependable for the purification of petroleum effluent as well as increasing the active area relatively with the working volume due to the finned modification of the cathode and tubular shape of the anodes.

Thankfulness

The researchers are grateful to the Al-Muthanna Petroleum Refinery (Production and Operation department and Technical Analyst of the Laboratory department).

Author's contribution

The article's concept and design, data analysis and interpretation, authorship, and final version approval were all contributed to by all of the authors. This particular paper has not yet been sent to any other journal or publication site, nor is it currently being reviewed by any of those places. The researchers have no financial ties to any entity referenced in this paper.

Table 5
Mathematical models of Inner and Outer anode consumption.

Responses	Mathematical correlations	R^2	R^2 (Adjusted)
Inner anode consumption	$Y = -0.0335 + 0.01655\ X_1 + 0.002452\ X_2 + 0.000089\ X_3 - 0.002417\ X_1^2 - 0.000024\ X_2^2 + 0.000000\ X_3^2 + 0.000123\ X_1 * X_2 - 0.000023\ X_1 * X_3 - 0.000003\ X_2 * X_3$ (Eq. 12)	0.9184	0.9709
Outer anode consumption	$Y = -0.1031 + 0.0283\ X_1 + 0.00578\ X_2 + 0.001247\ X_3 - 0.00393\ X_1^2 - 0.000027\ X_2^2 - 0.000005\ X_3^2 + 0.000163\ X_1 * X_2 - 0.000046\ X_1 * X_3 - 0.000023\ X_2 * X_3$ (Eq. 13)	0.9142	0.9694

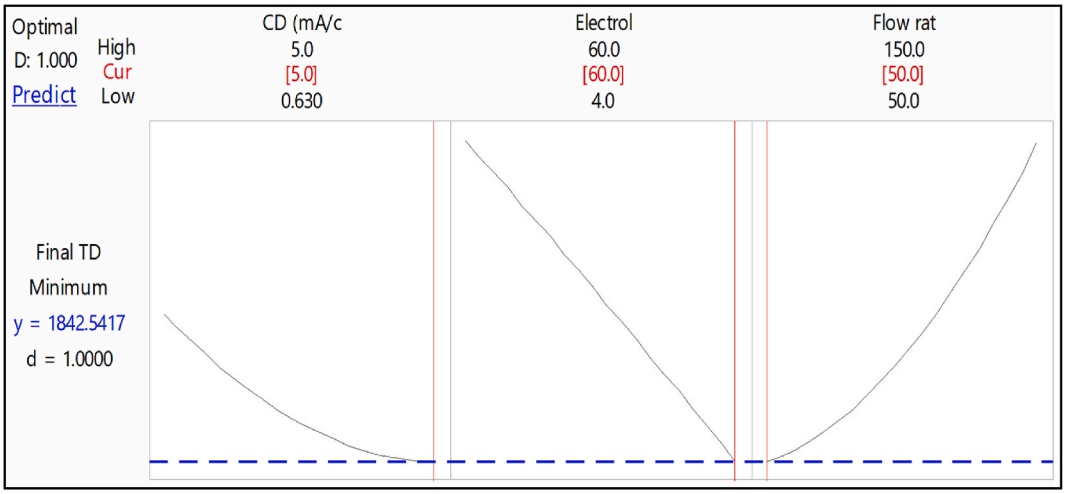

Fig. 9. The optimal values of the operating factor for the treated of TDS from petroleum wastewater.

Declaration of competing interest

The authors declare that they have no known competing financial interests or personal relationships that could have appeared to influence the work reported in this paper.

References

[1] N.M. Jabbar, S.M. Alardhi, T. Al-Jadir, H. Abed Dhahad, Contaminants removal from real refinery wastewater associated with energy generation in microbial fuel cell, J. Ecol. Eng. 24 (1) (2023) 107–114, https://doi.org/10.12911/22998993/156081.
[2] N.M. Jabbar, S.M. Alardhi, A.K. Mohammed, I.K. Salih, T.M. Albayati, Challenges in the implementation of bioremediation processes in petroleum-contaminated soils: a review, Environ. Nanotechnol. Monit. Manag. 18 (2022), 100694, https://doi.org/10.1016/j.enmm.2022.100694.
[3] F.Y. AlJaberi, Treatment of refinery wastewater by chemical advanced oxidation processes (UV-photolysis, fenton, and photo-fenton): a comparative study, Iran. J. Chem. Chem. Eng. (Int. Engl. Ed.) (2023), https://doi.org/10.30492/ijcce.2023.560200.5520.
[4] S.M. Alardhi, N.M. Jabbar, T. AL-Jadir, N.K. Ibrahim, A.M. Dakhil, N.D. Al-Saedi, H.D. Al-Saedi, M. Adnan, Artificial neural network model for predicting the desulfurization efficiency of Al-Ahdab crude oil, AIP Conf. Proc. 2443 (1) (2022), 030033, https://doi.org/10.1063/5.0091975.
[5] S.M. Alardhi, T. Al-Jadir, A.M. Hasan, A.A. Jaber, L.M. Al Saedi, Design of artificial neural network for prediction of hydrogen sulfide and carbon dioxide concentrations in a natural gas sweetening plant, Ecol. Eng. Environ. Tech. 24 (2) (2023) 55–66, https://doi.org/10.12912/27197050/157092.
[6] L. Tjale, H. Richards, O. Mahlangu, L.N. Nthunya, Silica nanoparticle modified polysulfone/polypropylene membrane for separation of oil-water emulsions, Results Eng. 16 (2022), 100623, https://doi.org/10.1016/j.rineng.2022.100623.
[7] M.A. Jasim, F.Y. AlJaberi, Treatment of oily wastewater by electrocoagulation technology: a general review (2018-2022): review paper, J. Electrochem. Sci. Eng. 13 (2) (2022) 361–372, https://doi.org/10.5599/jese.1472.
[8] B.H. Diya'uddeen, W.M.A.W. Daud, A.R. Abdul Aziz, Treatment technologies for petroleum refinery effluents: a review, Process Saf. Environ. Protect. 89 (2) (2011) 95–105, https://doi.org/10.1016/j.psep.2010.11.003.
[9] M.A. Jasim, F.Y. AlJaberi, Investigation of oil content removal performance in real oily wastewater treatment by electrocoagulation technology: RSM design approach, Results Eng. 18 (2023), 101082, https://doi.org/10.1016/j.rineng.2023.101082.
[10] F.Y. AlJaberi, S.A. Ahmed, H.F. Makki, Electrocoagulation treatment of high saline oily wastewater: evaluation and optimization, Heliyon 6 (6) (2020), https://doi.org/10.1016/j.heliyon.2020.e03988.
[11] M.H. El-Naas, S. Al-Zuhair, A. Al-Lobaney, S. Makhlouf, Assessment of electrocoagulation for the treatment of petroleum refinery wastewater, J. Environ. Manag. 91 (1) (2009) 180–185, https://doi.org/10.1016/j.jenvman.2009.08.003.
[12] M. Changmai, M. Pasawan, M.K. Purkait, Treatment of oily wastewater from drilling site using electrocoagulation followed by microfiltration, Separ. Purif. Technol. 210 (2019) 463–472, https://doi.org/10.1016/j.seppur.2018.08.007.
[13] T.K. Hussein, N.A. Jasim, A comparison study between chemical coagulation and electro-coagulation processes for the treatment of wastewater containing reactive blue dye, Mater. Today: Proc. 42 (2021) 1946–1950, https://doi.org/10.1016/j.matpr.2020.12.240.
[14] M.A. Jasim, F.Y. AlJaberi, P.C. Le, A.D. Salman, J. Miklos, B. Van, D. Duong La, S.W. Chang, D. Duc Nguyen, Investigating the influences of the cathode configuration on the electrocoagulation performance: a comparative study, Case Stud. Chem. Environ. Eng. 8 (2023), 100364, https://doi.org/10.1016/j.cscee.2023.100364.

[15] F.Y. AlJaberi, S.M. Alardhi, S.A. Ahmed, A.D. Salman, T. Juzsakova, I. Cretescu, P.-C. Le, W.J. Chung, S.W. Chang, D.D. Nguyen, Can electrocoagulation technology be integrated with wastewater treatment systems to improve treatment efficiency? Environ. Res. 214 (2022), 113890 https://doi.org/10.1016/j.envres.2022.113890.

[16] M.A. Jasim, F.Y. AlJaberi, Removal of COD from real oily wastewater by electrocoagulation using a new configuration of electrodes, Environ. Monit. Assess. 195 (651) (2023) 1–7, https://doi.org/10.1007/s10661-023-11257-y.

[17] G. Barzegar, J. Wu, F. Ghanbari, Enhanced treatment of greywater using electrocoagulation/ozonation: investigation of process parameters, Process Saf. Environ. Protect. 121 (2019) 125–132, https://doi.org/10.1016/j.psep.2018.10.013.

[18] N. Karimi, S.A. Mirbagheri, R. Nouri, A. Bazargan, Sequential application of aerated electrocoagulation and γ-Fe2O3 nanoparticle adsorption for COD removal: consuming the least amount of energy and economic evaluation, Results in Engineering 17 (2023), 100770, https://doi.org/10.1016/j.rineng.2022.100770.

[19] O. Ganzenko, D. Huguenot, E.D. van Hullebusch, G. Esposito, M.A. Oturan, Electrochemical advanced oxidation and biological processes for wastewater treatment: a review of the combined approaches, Environ. Sci. Pollut. Control Ser. 21 (14) (2014) 8493–8524, https://doi.org/10.1007/s11356-014-2770-6.

[20] F.Y. AlJaberi, S.A. Ahmed, H.F. Makki, A.S. Naje, H.M. Zwain, A.D. Salman, T. Juzsakova, S. Viktor, B. Van, P.C. Le, D.D. La, S.W. Chang, M.J. Um, H.H. Ngo, D. D. Nguyen, Recent advances and applicable flexibility potential of electrochemical processes for wastewater treatment, Sci. Total Environ. 867 (2023), 161361, https://doi.org/10.1016/j.scitotenv.2022.161361.

[21] H.P. de Carvalho, J. Huang, M. Zhao, G. Liu, L. Dong, X. Liu, Improvement of Methylene Blue removal by electrocoagulation/banana peel adsorption coupling in a batch system, Alex. Eng. J. 54 (3) (2015) 777–786, https://doi.org/10.1016/j.aej.2015.04.003.

[22] Y.-J. Liu, S.-L. Lo, Y.-H. Liou, C.-Y. Hu, Removal of nonsteroidal anti-inflammatory drugs (NSAIDs) by electrocoagulation–flotation with a cationic surfactant, Separ. Purif. Technol. 152 (2015) 148–154, https://doi.org/10.1016/j.seppur.2015.08.015.

[23] Y.F. AlJaberi, A.B. Abdulmajeed, A.A. Hassan, L.M. Ghadban, Assessment of an electrocoagulation reactor for the removal of oil content and turbidity from real oily wastewater using response surface method, Recent Innov. Chem. Eng. 13 (1) (2020) 55–71, https://doi.org/10.2174/2405520412666190830091842.

[24] F.Y.A. Jaberi, S.M. Jabbar, N.M. Jabbar, Modeling of adsorption isotherms of oil content through the electrocoagulation treatment of real oily wastewater, AIP Conf. Proc. 2213 (1) (2020), 020041, https://doi.org/10.1063/5.0000157.

[25] T. Al-Jadir, S.M. Alardhi, M.A. Alheety, A.A. Najim, I.K. Salih, M. Al-Furaiji, Q.F. Alsalhy, Fabrication and characterization of polyphenylsulfone/titanium oxide nanocomposite membranes for oily wastewater treatment, J. Ecol. Eng. 23 (12) (2022) 1–13, https://doi.org/10.12911/22998993/154770.

[26] L.S. Pérez, O.M. Rodriguez, S. Reyna, J.L. Sánchez-Salas, J.D. Lozada, M.A. Quiroz, E.R. Bandala, Oil refinery wastewater treatment using coupled electrocoagulation and fixed film biological processes, Phys. Chem. Earth, Parts A/B/C 91 (2016) 53–60, https://doi.org/10.1016/j.pce.2015.10.018.

[27] S.M. Alardhi, A.H. Abdalsalam, A.A. Ati, M.H. Abdulkareem, A.A. Ramadhan, M.M. Taki, Z.Y. Abbas, Fabrication of polyaniline/zinc oxide nanocomposites: synthesis, characterization and adsorption of methylene orange, Polym. Bull. (2023), https://doi.org/10.1007/s00289-023-04753-1.

[28] F. Ghanbari, M. Moradi, A comparative study of electrocoagulation, electrochemical Fenton, electro-Fenton and peroxi-coagulation for decolorization of real textile wastewater: electrical energy consumption and biodegradability improvement, J. Environ. Chem. Eng. 3 (1) (2015) 499–506, https://doi.org/10.1016/j.jece.2014.12.018.

[29] A.D. Salman, T. Juzsakova, S. Mohsen, T.A. Abdullah, P.-C. Le, V. Sebestyen, B. Sluser, I. Cretescu, Scandium recovery methods from mining, metallurgical extractive industries, and industrial wastes, Materials 15 (7) (2022) 2376, https://doi.org/10.3390/ma15072376.

[30] E. Gatsios, J.N. Hahladakis, E. Gidarakos, Optimization of electrocoagulation (EC) process for the purification of a real industrial wastewater from toxic metals, J. Environ. Manag. 154 (2015) 117–127, https://doi.org/10.1016/j.jenvman.2015.02.018.

[31] S. Elabbas, N. Ouazzani, L. Mandi, F. Berrekhis, M. Perdicakis, S. Pontvianne, M.N. Pons, F. Lapicque, J.P. Leclerc, Treatment of highly concentrated tannery wastewater using electrocoagulation: influence of the quality of aluminium used for the electrode, J. Hazard Mater. 319 (2016) 69–77, https://doi.org/10.1016/j.jhazmat.2015.12.067.

[32] C. Tsioptsias, D. Petridis, N. Athanasakis, I. Lemonidis, A. Deligiannis, P. Samaras, Post-treatment of molasses wastewater by electrocoagulation and process optimization through response surface analysis, J. Environ. Manag. 164 (2015) 104–113, https://doi.org/10.1016/j.jenvman.2015.09.007.

[33] V. Kuokkanen, T. Kuokkanen, J. Rämö, U. Lassi, J. Roininen, Removal of phosphate from wastewaters for further utilization using electrocoagulation with hybrid electrodes – techno-economic studies, J. Water Proc. Eng. 8 (2015) e50–e57, https://doi.org/10.1016/j.jwpe.2014.11.008.

[34] F.Y. AlJaberi, Removal of TOC from oily wastewater by electrocoagulation technology, IOP Conf. Ser. Mater. Sci. Eng. 928 (2) (2020), 022024, https://doi.org/10.1088/1757-899X/928/2/022024.

[35] F.Y. AlJaberi, Modelling current efficiency and ohmic potential drop in an innovated electrocoagulation reactor, Desalination Water Treat. 164 (2019) 102–110, https://doi.org/10.5004/dwt.2019.24452.

[36] F.Y. AlJaberi, Studies of autocatalytic electrocoagulation reactor for lead removal from simulated wastewater, J. Environ. Chem. Eng. 6 (5) (2018) 6069–6078, https://doi.org/10.1016/j.jece.2018.09.032.

[37] T.J. Mohammed, H.A. Al-Zuheri, Application of Response Surface Methodology for analysis and optimization of the operational parameters for turbidity removal from oily wastewater by electrocoagulation process, IOP Conf. Ser. Mater. Sci. Eng. 454 (1) (2018), 012069, https://doi.org/10.1088/1757-899X/454/1/012069.

[38] J. Schaep, B. Van der Bruggen, S. Uytterhoeven, R. Croux, C. Vandecasteele, D. Wilms, E. Van Houtte, F. Vanlerberghe, Removal of hardness from groundwater by nanofiltration, Desalination 119 (1) (1998) 295–301, https://doi.org/10.1016/S0011-9164(98)00172-6.

[39] W.-m. Jiang, Y.-m. Chen, M.-c. Chen, X.-l. Liu, Y. Liu, T. Wang, J. Yang, Removal of emulsified oil from polymer-flooding sewage by an integrated apparatus including EC and separation process, Separ. Purif. Technol. 211 (2019) 259–268, https://doi.org/10.1016/j.seppur.2018.09.069.

[40] F.Y. AlJaberi, Desalination of groundwater by electrocoagulation using a novel design of electrodes, Chem. Eng. Processing - Process Intensification 174 (2022), 108864, https://doi.org/10.1016/j.cep.2022.108864.

[41] H.K. Hansen, S.F. Peña, C. Gutiérrez, A. Lazo, P. Lazo, L.M. Ottosen, Selenium removal from petroleum refinery wastewater using an electrocoagulation technique, J. Hazard Mater. 364 (2019) 78–81, https://doi.org/10.1016/j.jhazmat.2018.09.090.

[42] M. Arellano, N. Oturan, M. Pazos, M. Ángeles Sanromán, M.A. Oturan, Coupling electro-Fenton process to a biological treatment, a new methodology for the removal of ionic liquids? Separ. Purif. Technol. 233 (2020), 115990 https://doi.org/10.1016/j.seppur.2019.115990.

[43] P. Patel, S. Gupta, P. Mondal, Electrocoagulation process for greywater treatment: statistical modeling, optimization, cost analysis and sludge management, Separ. Purif. Technol. 296 (2022), 115990.